Residual strain effects on the two-dimensional electron gas concentration of AlGaN/GaN heterostructures

G. Martínez-Criado,[a] A. Cros, and A. Cantarero
Materials Science Institute and Department of Applied Physics, University of Valencia, Dr. Moliner 50, 46100-Burjasot, Valencia, Spain

O. Ambacher, C. R. Miskys, R. Dimitrov, and M. Stutzmann
Walter Schottky Institute, Technical University Munich, Am Coulombwall, 85748-Garching, Germany

J. Smart and J. R. Shealy
School of Electrical Engineering, Cornell University, Ithaca, New York 14853

(Received 27 February 2001; accepted for publication 25 July 2001)

Ga-face AlGaN/GaN heterostructures with different sheet carrier concentrations have been studied by photoluminescence and Raman spectroscopy. Compared to bulk GaN, an energy shift of the excitonic emission lines towards higher energies was observed, indicating the presence of residual compressive strain in the GaN layer. This strain was confirmed by the shift of the E_2 Raman line, from which biaxial compressive stresses ranging between 0.34 and 1.7 GPa were deduced. The spontaneous and piezoelectric polarizations for each layer of the heterostructures have been also calculated. The analysis of these quantities clarified the influence of the residual stress on the sheet electron concentration (n_s). Possible causes for the discrepancies between the calculated and experimentally determined sheet carrier densities are briefly discussed. © *2001 American Institute of Physics.* [DOI: 10.1063/1.1408268]

I. INTRODUCTION

Group III nitrides materials offer great promise for high power, high frequency device applications, in particular for heterojunction field-effect transistors (FETs). III nitrides have several advantages over other material systems currently used for HFETs, such as a higher breakdown voltage, a better linearity, a lower phase noise, and higher thermal conductivity, all of which will allow a higher power-handling capability.[1,2] Although the AlGaAs/GaAs system offers higher two-dimensional electron gas drift mobilities for small electric fields, the electron saturation velocity in the AlGaN/GaN system is higher than in other III–V materials, allowing simultaneously high-frequency operation and high output power levels.[3,4]

In a typical modulation-doped FET structure the resulting band bending creates a triangular-well-like potential at the heterointerface, where the electrons accumulate forming a two-dimensional electron gas (2DEG). Since the lattice constant of GaN is larger than that of AlN by about 2.5%, $Al_{0.25}Ga_{0.75}N$ films with a thickness of up to 40 nm can be grown pseudomorphically on top of GaN buffer layers. In addition to the spontaneous polarization, which is different for AlGaN and GaN, the heteroepitaxial strain produces an additional macroscopic piezoelectric field contributing to the conduction band profile of the FET structure. Nominally undoped AlGaN/GaN transistors even exhibit a high sheet carrier density in the GaN channel as a consequence of polarization induced charges present at the heterointerface.[5,6] In this work, photoluminescence (PL) and Raman measurements on undoped and doped Ga face AlGaN/GaN transistor structures with sheet carrier concentrations ranging from 0.9 to $1.32\times10^{13}cm^{-2}$ are reported. The role of residual compressive strain detected by both types of experiments in the GaN layer of the heterostructures (HSs) on the sheet carrier concentration in the two-dimensional electron gas was analyzed.

II. EXPERIMENTAL DETAILS

The AlGaN/GaN heterostructures analyzed here were grown by metalorganic chemical vapor phase deposition (MOCVD) and plasma-induced molecular beam epitaxy (PIMBE) on *c*-plane sapphire (α-Al_2O_3) substrates. The MOCVD samples, A and B, were deposited at a pressure of 100 mbar, using triethylgallium (TEG), trimethylaluminium (TMA), and ammonia as precursors. A third HS, sample C, was grown by plasma induced molecular beam epitaxy. A more detailed description of the MOCVD and PIMBE systems, as well as growth conditions can be found in Refs. 5 and 7. In general, the samples have the following structure starting from the substrate: an initial AlN nucleation layer used to obtain Ga-face material,[7] followed by a GaN buffer layer and a strained AlGaN barrier layer. The PIMBE structure is capped by a 2 nm undoped GaN film, which turns out to be advantageous for HEMT devices based on AlGaN/GaN HSs.[8] For sample A, the AlGaN barrier is composed of 30 Å undoped $Al_{0.33}Ga_{0.67}N$ (spacer layer) followed by a Si-doped $Al_{0.33}Ga_{0.67}N$ layer of 120 Å thickness, and finally, 50 Å of undoped $Al_{0.33}Ga_{0.67}N$. From high resolution x-ray diffraction (HRXRD) measurements it was deduced that the AlGaN barriers grow pseudomorphically on the GaN layers, i.e., the lattice constants were identical within experimental accuracy.

[a]Electronic mail: gmc@uv.es

0021-8979/2001/90(9)/4735/6/$18.00 © 2001 American Institute of Physics

Downloaded 28 Jan 2010 to 147.156.182.23. Redistribution subject to AIP license or copyright; see http://jap.aip.org/jap/copyright.jsp

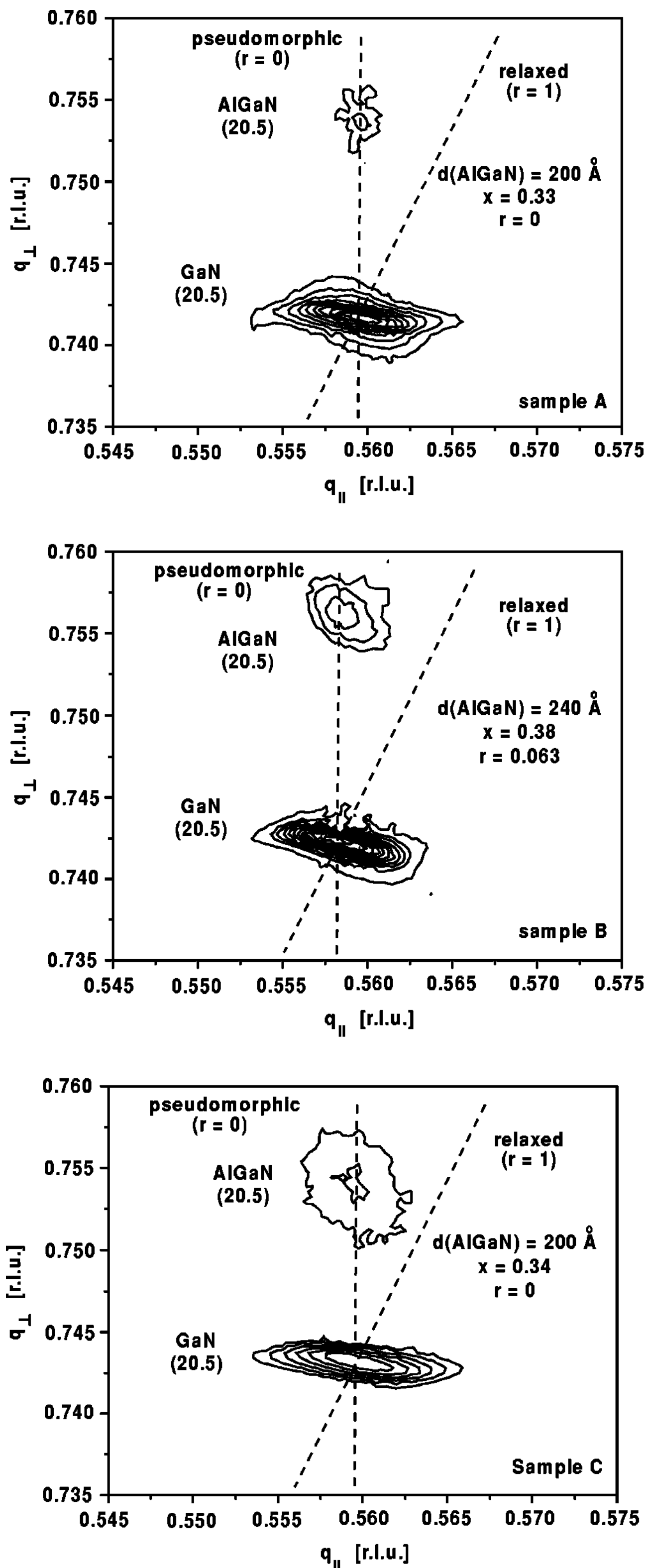

FIG. 1. Reciprocal space maps of (20.5) reflections of AlGaN/GaN heterostructures measured by HRXRD. The dashed lines show the position of the x-ray diffraction reflections for the relaxed and pseudomorphic grown AlGaN films.

The aluminum composition, x, and the degree of relaxation, r, were calculated from the lattice constants a and c determined by means of reciprocal space maps of the (20.5) reflection of AlGaN/GaN heterostructures (see Fig. 1).[5] Important parameters of the different samples are summarized in Table I.

Hall effect measurements have revealed sheet carrier concentrations and Hall mobilities at room temperature ranging from 0.9 to 1.32×10^{13}cm^{-2}, and from 1050 to 1532 cm^2 V^{-1} s^{-1}, respectively (Table I). Higher mobilities have been measured at low temperatures [$\mu(1.3\text{K})\approx 4500$ cm^2/V s], where the mobility is limited by scattering from impurities, defects, and/or interface roughness rather than phonons.[5] The observed thermal dependence, i.e., a significant increase of the electron mobilities with constant sheet electron concentration, is consistent with the spatial carrier confinement and the formation of a 2DEG.[4,7]

For PL measurements, the samples were mounted in a continuous He-flow cryostat operating at 4.3 K. For optical excitation different ultraviolet lines of an Ar^+ ion laser were used. The luminescence was detected with a 0.8 m DILOR triple spectrometer equipped with a cooled charge-coupled device detector. Micro-Raman experiments were carried out at low temperature (4.3 K) in the same system using the 514.5 nm line of the Ar^+ laser. The laser light was focused onto the sample with a 10× microscope objective.

III. RESULTS AND DISCUSSION

Photoluminescence spectra taken at low temperature for three Ga-face AlGaN/GaN HSs with different sheet carrier concentrations are shown in Fig. 2 on a logarithmic scale. The spectrum of a homoepitaxial GaN film is included as a reference. All spectra were measured with excitation energies below the AlGaN barrier band gap. The identification of all transitions was already made in a previous publication based on characteristic thermal and excitation power dependencies,[9] as well as on more recent high resolution PL studies.[10,11] The presence of free exciton lines in the MOCVD samples, A and B, together with the usual donor bound exciton transition confirms the high structural quality of these samples. In contrast, the MBE sample (C) only exhibits the donor bound exciton line at 3.496 eV with a full width at half maximum (FWHM) of 11 meV, suggesting lower heterojunction quality. The structural quality of the heterojunction plays an important role in the achieved carrier mobility, as can be seen from the Hall results shown in Table I. Finally, it is important to mention the collective shift of the optical transitions in all HSs towards higher energies in comparison to the reference sample. This behavior is attributed to residual compressive strain in the GaN layer caused by lattice mismatch and differences in the thermal expansion coefficients between film and substrate.

The abovementioned residual compressive strain in the GaN buffer layer has been confirmed by means of Raman measurements of the E_2 phonon mode, which is known to be shifted by stress only[12] (Fig. 3). Using the relationship reported by Demangeot *et al.*[13] for the dependence of the E_2-phonon frequency on biaxial compressive stress in GaN layers:

$$\Delta\omega = C\cdot\sigma_{xx}, \tag{1}$$

Downloaded 28 Jan 2010 to 147.156.182.23. Redistribution subject to AIP license or copyright; see http://jap.aip.org/jap/copyright.jsp

TABLE I. Summary of relevant parameters of the Ga-face AlGaN/GaN heterostructures investigated in this work. In sample A the AlGaN barrier consists of 30 Å of undoped $Al_{0.30}Ga_{0.70}N$ followed by Si-doped $Al_{0.33}Ga_{0.67}N$ ($[Si]=1\times10^{19}$ cm^{-3}) of 120 Å thickness, and 50 Å of undoped $Al_{0.33}Ga_{0.67}N$. μ_s and n_s are the sheet carrier mobility and density, respectively.

		GaN cap layer	AlGaN barrier		GaN buffer	Hall data at 300 K	
Sample	Growth method	d (Å)	x	d (Å)	d μm	μ_s ($cm^2/V\,s$)	n_s (10^{13} cm^{-2})
A	MOCVD		0.33	200	2	1100	1.32
B	MOCVD		0.38	240	3	1532	1.05
C	MBE	25	0.34	200	2	1050	0.90

where $C=-(2.9\pm0.3)$ $cm^{-1}\,GPa^{-1}$, we obtain residual compressive stresses ranging from 0.34 to 1.7 GPa. The intrinsic value of $\omega_{E_2(\mathrm{high})}=568$ cm^{-1} was taken from the reference homoepitaxial GaN film. We have neglected any possible additional hydrostatic stress components induced by point defects. The linewidth of the GaN E_2 mode line of the AlGaN layer is associated with compositional disorder.[14] Since the penetration depth of the 514.5 nm argon line used for Raman scattering is larger than that of the 333.6 nm line, we will just use the PL results to examine the region close to the heterointerface. Applying the expression reported by Rieger *et al.*[15] for the bound exciton energy shift of GaN films grown on AlN nucleation layers;

$$\Delta E_{DX}=B\cdot\sigma_{xx}, \tag{2}$$

where $B=(27\pm4)$ meV GPa^{-1}, biaxial compressive stresses between 0.10 and 0.79 GPa are obtained. As reference we have taken the donor bound exciton transition of the homoepitaxial GaN film centered at 3.4747 eV. The difference between the Raman and PL strain results is a consequence of strain relaxation with increasing layer thickness.

With the purpose of analyzing the effects of this compressive strain of the GaN buffer layers on the 2DEG concentration, Fig. 4 shows a schematic diagram of the piezoelectric and spontaneous polarization vectors for a Ga-face AlGaN layer grown pseudomorphically on top of a GaN layer in the (0001) orientation with the wurtzite crystal structure. Associated with this spatial gradient of polarization there is an induced fixed atomic charge density given by $\rho_P=-\nabla\mathbf{P}$. If the GaN layer additionally is under compressive strain, it could be expected by elementary vector analysis that its piezoelectric polarization (Fig. 4), given by:[6,5]

$$P^{*}_{\mathrm{PE}}=2\varepsilon_{xx}(e_{31}-e_{33}C_{13}/C_{33}) \tag{3}$$

would increase the sheet electron concentration at the interface, since $(e_{31}-e_{33}C_{13}/C_{33})<0$. In the former expression, e_{13} and e_{33} are the piezoelectric coefficients, ε_{xx} the in-plane component of the strain tensor, and C_{13} and C_{33} are components of the compliance tensor. Consequently, the most strongly compressed GaN layer should apparently present the highest induced electric field, as well as the highest sheet charge density at the interface. However, we have just obtained the opposite result: the least strained GaN layer, sample A, has the highest sheet carrier Hall concentration, $n_s=1.32\times10^{13}$ cm^{-2}. One can argue that the Si-doped $Al_{0.30}Ga_{0.70}N$ film present in the AlGaN barrier of sample A increases the electron density in the GaN layer compared to the other two samples by transfer doping. However, this only explains our results partially; as was already demonstrated in a previous study,[6] the formation of 2DEGs in undoped as well as doped AlGaN/GaN structures is almost completely dominated by piezoelectric and spontaneous polarization induced effects.

Therefore, for a more thorough discussion of our Hall results, the sheet carrier concentration values taking into ac-

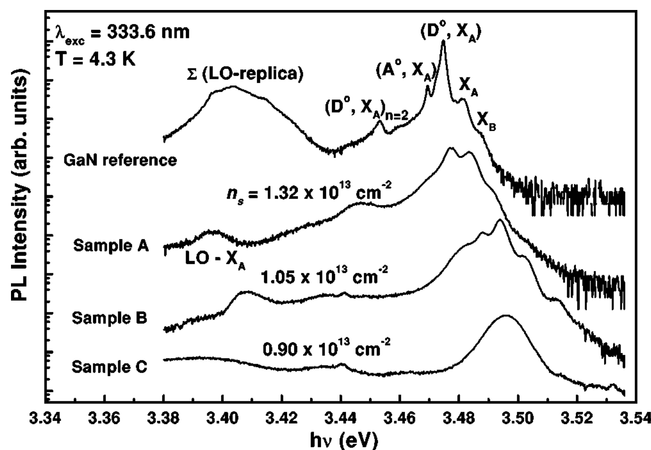

FIG. 2. Photoluminescence spectra taken at 4.3 K for Ga-face SHs with different sheet carrier concentrations. Samples A, B have been grown by MOCVD, and C is an MBE sample.

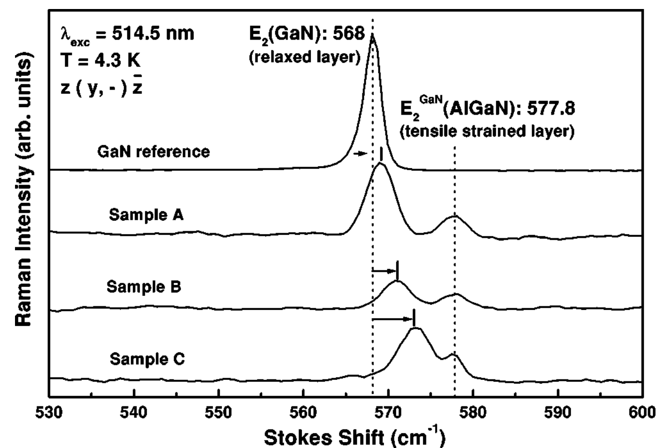

FIG. 3. Micro-Raman spectra taken at low temperature. The assignment of the phonon modes is indicated in each spectrum.

Downloaded 28 Jan 2010 to 147.156.182.23. Redistribution subject to AIP license or copyright; see http://jap.aip.org/jap/copyright.jsp

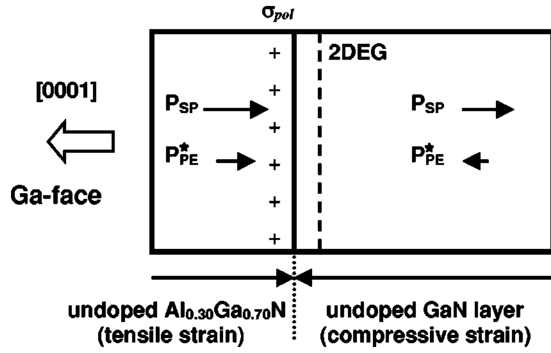

FIG. 4. Directions of the spontaneous and piezoelectric polarizations for the Ga-face strained AlGaN/GaN HS with a residual compressive strain presents in the GaN layer.

count the experimentally determined compressive strain will be determined. The normal (ε_{zz}) and in-plane (ε_{xx}) components of the strain tensor have been calculated using the model of a biaxially strained layer ($\sigma_{xy}=\sigma_{xz}=\sigma_{yz}=0$; $\sigma_{xx}=\sigma_{yy}$):[16]

$$\varepsilon_{xx}=\varepsilon_{yy}=\left(\frac{C_{33}}{(C_{11}+C_{12})C_{33}-2C_{13}^2}\right)\sigma_{xx},$$

and

$$\varepsilon_{zz}=-2\frac{C_{13}}{C_{33}}\varepsilon_{xx}. \tag{4}$$

Since the AlGaN barriers were grown pseudomorphically on top of GaN, their lattice constants are identical at the heterointerface, i.e., $a(\mathrm{AlGaN}) = a(\mathrm{GaN})$. Therefore, the AlGaN lattice constant was determined through the relation $a_{\mathrm{AlGaN}}=a_0(1-\varepsilon_{xx})=a_{\mathrm{GaN}}$, where a_0 is the unstrained GaN lattice constant and ε_{xx} is the strain in the GaN buffer. The components of the strain tensor for the AlGaN layer were calculated using elastic constants determined from linear interpolations between GaN and AlN binary ends.[5] The obtained values for σ_{xx}, ε_{xx}, and ε_{zz} are listed in Table II for the set of samples used in this work.

Counting the energy from the bottom of the conduction band at the interface for an $\mathrm{Al}_x\mathrm{Ga}_{1-x}\mathrm{N}$/GaN HS, where the AlGaN barrier is composed by 30 Å of undoped $\mathrm{Al}_{0.33}\mathrm{Ga}_{0.67}\mathrm{N}$ spacer followed by a Si-doped $\mathrm{Al}_{0.33}\mathrm{Ga}_{0.67}\mathrm{N}$ layer ($[\mathrm{Si}]=1\times10^{19}\ \mathrm{cm}^{-3}$) of 120 Å thickness, and 50 Å of undoped $\mathrm{Al}_{0.33}\mathrm{Ga}_{0.67}\mathrm{N}$ layer (sample A), one obtains the implicit equation in n_s:

$$\Delta E_c(x)=E_F(x)+e\phi_b(x)-\frac{N_d d_{dop}e^2}{\epsilon_0\epsilon(x)}\left(d_{sp}+\frac{d_{dop}}{2}\right)-\frac{d_{\mathrm{AlGaN}}e^2}{\epsilon_0\epsilon(x)}\left(\frac{+\sigma}{e}-n_s(x)\right), \tag{5}$$

and consequently, the maximum value of n_s can be calculated. In Eq. (5) N_d is the doping concentration in the Si-doped AlGaN layer, d_{sp}, d_{dop}, and d_{AlGaN} are the thicknesses of the spacer layer, the Si-doped layer, and the total AlGaN barrier, respectively. In addition, $e\phi_b$ is the Schottky barrier height of the gate contact on top of the AlGaN layer, ΔE_c the conduction band offset at the heterointerface, and E_F the Fermi level relative to the GaN conduction-band edge:

$$E_F(x)=E_0(x)+\frac{\pi\hbar^2 n_s(x)}{m^*}, \tag{6}$$

where we have assumed the ground energy level of a semi-infinite asymmetric triangular well, expressed by:

$$E_0(x)=\frac{3}{4}\left(\frac{\hbar^2}{2m^*}\right)^{1/3}\left(\frac{3\pi^2 n_s(x)}{2\epsilon_0\epsilon(x)}\right)^{2/3}. \tag{7}$$

The piezoelectrically induced polarization charge density at the interface σ is given by

$$\sigma=[P_{\mathrm{SP}}(\mathrm{AlGaN})+P_{\mathrm{PE}}^*(\mathrm{AlGaN})]-[P_{\mathrm{SP}}(\mathrm{GaN})+P_{\mathrm{PE}}^*(\mathrm{GaN})], \tag{8}$$

where P_{SP} is the spontaneous polarization. To determine the band offset, we use the approximation:[5] $\Delta E_c(x)=0.7[E_g(x)-E_g(0)]$, where the experimentally determined band gap of $\mathrm{Al}_x\mathrm{Ga}_{1-x}\mathrm{N}$ alloy at room temperature is given by:[17]

$$E_g(x)=6.13x+3.42(1-x)-1.0(1-x)x(\mathrm{eV}). \tag{9}$$

For sample B, where both the AlGaN barrier and the GaN layers are nominally undoped, Eq. (5) is reduced to:[5]

$$\Delta E_c(x)=E_F(x)+e\phi_b(x)-\frac{d_{\mathrm{AlGaN}}e^2}{\epsilon_0\epsilon(x)}\left(\frac{+\sigma}{e}-n_s(x)\right). \tag{10}$$

Finally, in the case of the same nominally undoped structure but with a GaN cap layer on top of it, as it is the case for sample C, Eq. (5) can be rewritten as:

TABLE II. Calculated stress, in-plane component of the strain tensor, spontaneous and piezoelectric polarizations, induced polarization charge density, and sheet carrier concentration of the different SHs.

Sample	E_{DX} (eV)	$\sigma_{xx}^{\mathrm{GaN}}$ (GPa)	$\varepsilon_{xx}^{\mathrm{GaN}}$ (%)	$P_{\mathrm{PE}*}^{\mathrm{GaN}}$ (10^{-7} C/cm^2)	$P_{\mathrm{PS}}^{\mathrm{GaN}}$ (10^{-6} C/cm^2)	$\varepsilon_{xx}^{\mathrm{AlGaN}}$ (%)	$P_{\mathrm{PE}*}^{\mathrm{AlGaN}}$ (10^{-6} C/cm^2)	$P_{\mathrm{PS}}^{\mathrm{AlGaN}}$ (10^{-6} C/cm^2)	σ (10^{-6} C/cm2)	n_s[a] (10^{13} cm^{-2})	n_s[b] (10^{13} cm^{-2})
A	3.4774	−0.10	−0.022	0.300	−2.9	0.781	−1.2245	−4.616	2.971	2.232	2.235
B	3.4937	−0.70	−0.156	2.107	−2.9	0.678	−1.2309	−4.876	3.418	2.005	2.031
C	3.4960	−0.79	−0.176	2.377	−2.9	0.650	−1.0239	−4.668	3.030	1.688	1.712

[a]Strained GaN buffer layer.
[b]Relaxed GaN buffer layer.

Downloaded 28 Jan 2010 to 147.156.182.23. Redistribution subject to AIP license or copyright; see http://jap.aip.org/jap/copyright.jsp

TABLE III. Linear interpolations between GaN and AlN binary properties ($T=300$ K) (Ref. 5).

	GaN	AlN	$Al_xGa_{1-x}N$
a_0 (Å)	3.189	3.112	$3.189-0.077x$
C_{11} (GPa)	367	396	367 + 29 x
C_{12} (GPa)	135	137	$135+2x$
C_{13} (GPa)	103	108	$103+5x$
C_{33} (GPa)	405	373	$405-32x$
e_{31} (C/m^2)	-0.49	-0.6	$-0.49-0.11x$
e_{33} (C/m^2)	0.73	1.46	$0.73+0.73x$
ϵ	9.5	9.0	$9.5-0.5x$
$e\phi_b$ (eV)[a]	0.84	2.14	$0.84+1.3x$

[a]Schottky barrier height for HSs without GaN-cap layer.

$$\Delta E_c(x)=E_F(x)+e\phi_b^{\text{eff}}(x)-\frac{d_{\text{AlGaN}}e^2}{\epsilon_0\epsilon(x)}\times\left(\frac{+\sigma}{e}-n_s(x)\right), \tag{11}$$

where $e\phi_b^{\text{eff}}$ is the effective barrier height given by

$$e\phi_b^{\text{eff}}(x)=e\phi_b^{\text{GaN}}+\Delta E_c(x)+\frac{d_{\text{GaN}}n_se^2}{\epsilon_0\epsilon(0)}. \tag{12}$$

The thickness of the cap layer is d_{GaN}, and $e\phi_b^{\text{GaN}}$ represents the Schottky barrier height of the gate contact on top of this GaN layer. The background dopant concentration in all layers, except for the Si-doped AlGaN layer in sample A, is assumed to be negligibly small in comparison to the polarization induced charge concentrations. All the calculated parameters are summarized in Table II. We use the set of linear interpolations between the physical properties of GaN and AlN at room temperature reported in Ref. 5 (see Table III). The change of strain and ΔP_{PE}^* due to thermal disagreement between optical measurements ($T=4$ K) and the Hall measurements to determine n_s ($T=300$ K), taking into account the difference in thermal expansion coefficients α between AlGaN and GaN layers, could be estimated by means of the expression:[18]

$$\Delta\varepsilon_{xx}=\frac{(\alpha_{\text{AlGaN}}-\alpha_{\text{GaN}})\Delta T}{1+\alpha_{\text{AlGaN}}\Delta T}. \tag{13}$$

A change of in-plane strain of about $\Delta\varepsilon_{xx}=0.012\%$ is obtained for the $Al_{0.30}Ga_{0.70}N$ layer, whereas this is compressive strain in the GaN layer because it has a larger expansion coefficient than AlN. However, this result would only lightly change the net residual compressive strain present in the GaN buffer layer.

The piezoelectric polarization in the GaN layer increases with compressive stress. This simultaneously causes a reduction of the tensile stress in the pseudomorphically grown AlGaN film, and consequently, a decrease of its piezoelectric polarization as shown in Fig. 5. Since the slopes of the piezoelectric polarization curves as a function of the in-plane strain are very similar for both materials [$P_{\text{PE}}^{\text{GaN}}(\text{C/cm}^2)=-1.353\times10^{-6}\ \varepsilon_{xx}^{\text{GaN}}$ vs $P_{\text{PE}}^{\text{Al}_{0.30}\text{Ga}_{0.70}\text{N}}(\text{C/cm}^2)=-1.547\times10^{-6}\ \varepsilon_{xx}^{\text{Al}_{0.30}\text{Ga}_{0.70}\text{N}}$], the net effect of the residual compressive strain on the Ga-face HSs is a small reduction of the polarization induced charge densities σ at the interface (Table II).

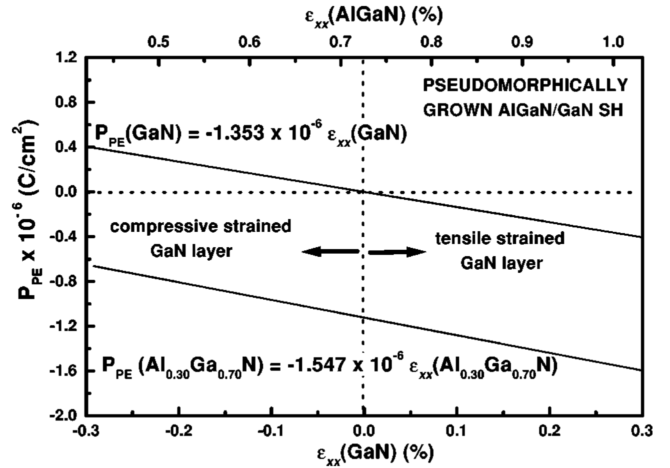

FIG. 5. Piezoelectric polarization for both layers (AlGaN and GaN) as a function of the in-plane strain.

For a wider range of in-plane strain in the GaN buffer layer, Fig. 6 shows the calculated sheet carrier concentration for different alloy composition in the case of a B-type SH. As the aluminum content increases in the barrier, the net effect of a residual compressive stress [$\varepsilon_{xx}(\text{GaN})<0$] becomes evident decreasing the 2DEG concentration at the heterointerface. On the contrary, for tensile strain [$\varepsilon_{xx}(\text{GaN})>0$] there will be a monotonous increasing with barrier composition. In any case, Fig. 6 demonstrates the definitive influence of residual strain on the sheet carrier concentration. A closer insight into Table II shows that there are small but clear

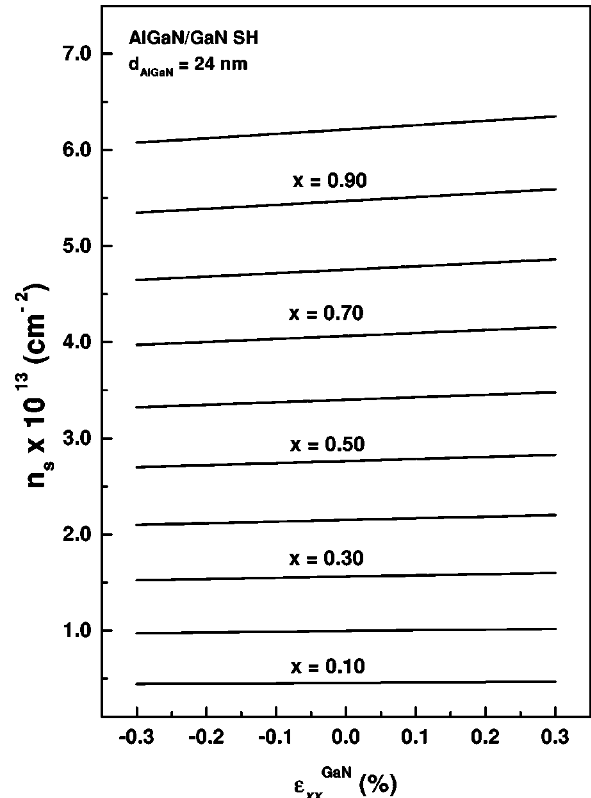

FIG. 6. Sheet carrier concentration of the 2DEG confined by polarization effects at an AlGaN/GaN interface as a function of the in-plane GaN strain.

Downloaded 28 Jan 2010 to 147.156.182.23. Redistribution subject to AIP license or copyright; see http://jap.aip.org/jap/copyright.jsp

differences between the relaxed and compressive strained GaN buffer layer cases, n_s^a and n_s^b. In spite of this result, the residual compressive strain does not explain the differences found between the sheet carrier concentration measured by Hall effect and the calculated values listed in Table II. These discrepancies can be caused by many other factors. For instance, it has been shown experimentally that in modulation-doped *n*-type AlGaAs/GaAs single heterojunctions fewer electrons are transferred than theoretically predicted, but no generally accepted explanation of this phenomenon has been provided. In spite of all the uncertainties on the material parameters used in our calculations we can attempt to explain our data taking into account some prior results for the AlGaAs system. For example, compensation of the AlGaN barrier material can contribute to the discrepancy between the measurements and calculations. Another feature is the erratic residual doping in the GaN channel, which could be a limiting factor in these samples. Additionally, the presence of deep traps in AlGaN could have a strong influence, since they may involve complexes whose activation energy depends on their charge state. This occurs in the same way for the traps responsible for the persistent photoconductivity phenomenon in the AlGaAs system.

On the other hand, as was shown in a previous work for an abrupt and flat interface, solving Schrödinger's and Poisson's equations self-consistently and taking the polarization induced interface charges into account, the maximum 2DEG density is quite sensitive to strain field and alloy barrier composition.[6] Hence, if alloy disorder, nonuniform strain fields, mixed polarities, interface roughness, and/or other structural defects (such as dislocations, inversion domains, etc.) are present at the heterointerface, they will alter appreciably the transfer of electrons from the $Al_{0.30}Ga_{0.70}N$ film to the GaN layer, leading to a reduction of the 2DEG sheet carrier concentration. Finally, very complete energy-level calculations, including interface grading, nonzero temperature, finite-barrier effects, effective mass, dielectric constant discontinuities, etc., are necessary. In a similar manner, more refined calculations of the electrostatic potentials taking into account compensation and residual doping of the various layers, Fermi level pinning, strain gradients, etc., should be performed.

IV. CONCLUSIONS

We have investigated Ga-face AlGaN/GaN HSs by means of PL and Raman measurements. A compressive stress is induced in the GaN layer by lattice mismatch and differences in thermal expansion coefficients between film and substrate. Its values were determined by Raman measurements as well as PL energy shifts. From our study we clarified the role of this compressive stress on the sheet carrier concentration at the AlGaN/GaN heterointerface. Finally, the possible causes of the discrepancies between the calculated and experimentally determined n_s have been briefly discussed.

ACKNOWLEDGMENTS

G. M.-C. would like to thank the Agencia Española de Cooperación Internacional (AECI) for granting her fellowship, as well as the Generalitat Valenciana for continuous support. In the same way, A. C. gratefully acknowledges financial support under Grant No. GV00-080-15 and MAT2000-0772.

[1] Y.-F. Wu, B. P. Keller, S. Keller, D. Kapolnek, P. Kozodoy, S. P. DenBaars, and U. K. Mishra, Appl. Phys. Lett. **69**, 1438 (1996).
[2] Y.-F. Wu, B. P. Keller, S. Keller, N. X. Nguyen, M. L. C. Nguyen, T. J. Jenkins, S. P. DenBaars, and U. K. Mishra, IEEE Electron Device Lett. **18**, 438 (1997).
[3] R. Gaska, J. W. Yang, A. Osinsky, Q. Chen, M. Asif Khan, A. O. Orlov, G. L. Snider, and M. S. Shur, Appl. Phys. Lett. **72**, 707 (1998).
[4] O. Ambacher, J. Phys. D **31**, 2653 (1998).
[5] O. Ambacher, J. Smart, J. R. Shealy, N. G. Weimann, K. Chu, M. Murphy, W. J. Schaff, L. F. Eastman, R. Dimitrov, L. Wittmer, and M. Stutzmann, J. Appl. Phys. **85**, 3223 (1999).
[6] O. Ambacher, B. Foutz, J. Smart, J. R. Shealy, N. G. Weimann, K. Chu, M. Murphy, A. J. Sierakowski, W. J. Schaff, L. F. Eastman, R. Dimitrov, A. Mitchell, and M. Stutzmann, J. Appl. Phys. **87**, 334 (2000).
[7] R. Dimitrov, L. Wittmer, H. P. Felsl, A. Mitchell, O. Ambacher, and M. Stutzmann, Phys. Status Solidi A **168**, R7 (1998).
[8] E. T. Yu, Z. Dang, L. S. Yu, D. Qiao, P. M. Asbeck, S. S. Lau, G. J. Sullivan, K. S. Boutros, and J. M. Redwing, Appl. Phys. Lett. **73**, 1880 (1998).
[9] G. Martínez-Criado, A. Cros, A. Cantarero, O. Ambacher, C. R. Miskys, R. Dimitrov, and M. Stutzmann, Phys. Rev. B (to be published).
[10] K. Korntizer, T. Ebner, K. Thonke, R. Sauer, C. Kirchner, V. Schwegler, M. Kamp, M. Leszczynski, I. Grzegory, and S. Porowski, Phys. Rev. B **60**, 1471 (1999).
[11] B. J. Skromme, J. Jayapalan, R. P. Vaudo, and V. M. Phanse, Appl. Phys. Lett. **74**, 2358 (1999).
[12] P. Perlin, C. Jauberthie-Carllon, J. P. Itie, A. S. Miguel, I. Grzegory, and A. Polian, Phys. Rev. B **45**, 83 (1992).
[13] F. Demangeot, J. Frandon, M. A. Renucci, O. Briot, B. Gil, and R. L. Aulombard, Solid State Commun. **100**, 207 (1996).
[14] A. Cros, H. Angerer, O. Ambacher, M. Stutzmann, R. Höpler, and T. Metzger, Solid State Commun. **104**, 35 (1997).
[15] W. Rieger, T. Metzger, H. Angerer, R. Dimitrov, O. Ambacher, and M. Stutzmann, Appl. Phys. Lett. **68**, 970 (1996).
[16] D. R. Lovett, in *Tensor Properties of Crystals* (Institute of Physics Publishing Ltd. London, 1989).
[17] D. Brunner, H. Angerer, E. Bustarret, R. Höpler, R. Dimitrov, O. Ambacher, and M. Stutzmann, J. Appl. Phys. **82**, 5090 (1997).
[18] G. Steude, B. K. Meyer, A. Göldner, A. Hoffmann, A. Kaschner, F. Bechstedt, H. Amano, and I. Akasaki, Jpn. J. Appl. Phys., Part 2 **38**, L498 (1999).

Downloaded 28 Jan 2010 to 147.156.182.23. Redistribution subject to AIP license or copyright; see http://jap.aip.org/jap/copyright.jsp